Gab2 promotes the growth of colorectal cancer by regulating the M2 polarization of tumor-associated macrophages

XUEHAN GAO[1,2*], RUNYING LONG[1-3*], MING QIN[1,2], WENFANG ZHU[4], LINNA WEI[1,2], PINZHI DONG[1,2], JIN CHEN[1,2], JUNMIN LUO[1,2] and JIHONG FENG[4]

[1]Special Key Laboratory of Gene Detection and Therapy and Base for Talents in Biotherapy of Guizhou Province; [2]Department of Immunology, Zunyi Medical University, Zunyi, Guizhou 563000; [3]Department of Obstetrics and Gynaecology, School of Clinical Medicine, Li Ka Shing Faculty of Medicine, The University of Hong Kong, Hong Kong, SAR 999077; [4]Department of Oncology, Lishui People's Hospital, Sixth Affiliated Hospital of Wenzhou Medical University, Lishui, Zhejiang 323000, P.R. China

Abstract. Tumor-associated macrophages (TAMs) are pivotal components in colorectal cancer (CRC) progression, markedly influencing the tumor microenvironment through their polarization into the pro-inflammatory M1 or pro-tumorigenic M2 phenotypes. Recent studies have highlighted that the Grb2-associated binder 2 (Gab2) is a critical gene involved in the development of various types of tumor, including CRC. However, the precise role of Gab2 in mediating TAM polarization remains incompletely elucidated. In the present study, it was discovered that Gab2 was highly expressed within CRC tissue TAMs, and was associated with a poor prognosis of patients with CRC. Functionally, it was identified that the tumor-conditioned medium (TCM) induced Gab2 expression, facilitating the TAMs towards an M2-like phenotype polarization. Of note, the suppression of Gab2 expression using shRNA markedly inhibited the TCM-induced expression of M2-associated molecules, without affecting M1-type markers. Furthermore, the xenotransplantation model demonstrated that Gab2 deficiency in TAMs inhibited tumor growth in the mouse model of CRC. Mechanistically, Gab2 induced the M2 polarization of TAMs by regulating the AKT and ERK signaling pathways, promoting CRC growth and metastasis. In summary, the present study study elucidates that decreasing Gab2 expression hinders the transition of TAMs towards the M2 phenotype, thereby suppressing the growth of CRC. The exploration of the regulatory mechanisms of Gab2 in TAM polarization may enhance the current understanding of the core molecular pathways of CRC development and may thus provide a foundation for the development of novel immunotherapeutic strategies targeted against TAMs.

Correspondence to: Dr Junmin Luo, Department of Immunology, Zunyi Medical University, 6 Xuefu West Road, Xinpu New District, Zunyi, Guizhou 563000, P.R. China
E-mail: luojm16128@163.com

Dr Jihong Feng, Department of Oncology, Lishui People's Hospital, Sixth Affiliated Hospital of Wenzhou Medical University, 1188 Liyang Street, Liandu, Lishui, Zhejiang 323000, P.R. China
E-mail: jh_f@163.com

*Contributed equally

Introduction

Colorectal cancer (CRC) is the third most frequent type of cancer worldwide and one of the most common malignant tumors of the digestive tract. According to the International Agency for Research on Cancer (IARC) data, there were ~1.93 million new cases in 2020, with 935,000 related deaths (1,2). The onset of CRC is a complex developmental process involving numerous phases and the involvement of multiple genes, with atypical early symptoms. Traditional treatment procedures, such as surgery, chemoradiotherapy and targeted therapy have gained some success; however, patient survival rates after 5 years are not yet optimal (3,4). Therefore, it is crucial to explore the pathogenesis of CRC and to identify novel therapeutic targets for the diagnosis and treatment of CRC.

The environment in which the tumor cells are positioned affects the growth of tumors in addition to the

genomic instability and epigenetic alterations of the tumor itself (5,6). Tumor cells, non-tumor stromal cells (endothelial cells, tumor-associated fibroblasts and immune cells) and extracellular components (extracellular matrix, growth factors, cytokines, etc.) comprise the majority of the tumor microenvironment (TME), which is the term used to describe the mesenchymal cells that the tumor locally infiltrates. Chemokines produced by tumor cells have the capacity to facilitate blood vessel formation (7-9). Tumor-associated macrophages (TAMs) are macrophages are considered to be the most numerous and significant proportion of myeloid cells in the TME. As one of the key elements of the TME, TAMs are closely linked to the development of tumor-associated inflammation (10,11). TAMs can affect tumor growth, invasion and metastasis, as well as vascular formation within the tumor. Furthermore, TAMs can suppress the development of the antitumor immune response by secreting a variety of cytokines and chemokines, thus playing a multifaceted role in shaping the context of tumor development and progression (12,13).

Within the TME, TAMs are stimulated by various signals, undergoing polarization into the distinct subtypes, M1 and M2. The activation of M1-type macrophages, triggered by molecules, such as lipopolysaccharide (LPS) and interferon-γ (IFN-γ), is associated with the antitumor response. Conversely, the generation of M2-type macrophages, mainly induced by interleukin (IL)-4 and IL-13, promotes tumor immune escape, highlighting a crucial role of this type of TAMs in cancer progression (14,15). TAMs are generally M2-type macrophages and are associated with malignant disease progression, drug resistance, recurrence and metastasis, as well as with a poor prognosis (16,17). Therefore, the identification and development of targets capable of modulating the polarization state of TAMs may prove to be a pivotal strategy with which to limit tumor growth and proliferation.

Grb2-associated binder 2 (Gab2) is one of the crucial members of the Gab protein family. This family of proteins represents a class of substrate molecules that can associate with tyrosine kinase through the recruitment of signaling molecules rich in phosphotyrosine domains, participating in the activation and transduction of numerous signaling pathways, playing a critical role in cellular physiological processes, such as differentiation, proliferation, migration and apoptosis (18). Previous studies have discovered a marked elevated expression of Gab2 in leukemia (19,20) and several human malignancies, such as breast cancer (BRCA) (21), ovarian cancer (OV) (22,23), hepatocellular carcinoma (HCC) (24,25), CRC (26) and melanoma (27), indicating its potential significance in oncologic progression. However, the impact and mechanisms of action of Gab2 on TAM polarization remain unclear. Thus, further exploration is required in order to elucidate its complex role within the TME.

The present study aimed to investigate the following: i) The expression level of Gab2 within TAMs in tissue microarrays from patients with CRC, and its association with patient survival; ii) the effect of Gab2 on TAM polarization *in vitro*; and iii) verify the potential role of Gab2 in modulating TAM polarization and its effects on CRC progression, by utilizing a mouse subcutaneous transplantation model.

Materials and methods

Tissue microarray and fluorescence staining. Human CRC tissue microarrays (cat. no. HColA180Su12) that included 93 paraffin-embedded CRC tissues and 87 para-cancerous tissues were obtained from Shanghai Outdo Biotech Co., Ltd. The present study was approved by the Ethics Committee of the Shanghai Outdo Biotech Co., Ltd., and was conducted in accordance with the ethical standards set out in the Declaration of Helsinki. All patients or their next of kin provided their informed consent prior to the study.

The tissue microarrays were dewaxed and hydrated; antigen retrieval was performed by boiling the tissue sections in 10 mM sodium citrate buffer with pH 6.0 at 100°C for 10 min. Following this, the tissue sections were blocked and then incubated overnight at 4°C with the corresponding primary antibodies. The following antibodies were used in the present study: CD68 (1:100; cat. no. ab283654; Abcam), Gab2 (1:50; cat. no. 22549-1-AP; Proteintech Group, Inc.). The tissue sections were then washed three times with TBST for 5 min each. This was followed by a 2-h incubation at room temperature in the dark with the following secondary antibodies: Alexa Fluor 488-conjugated goat anti-rabbit IgG (H+L) (1:500; cat. no. 4412; Cell Signaling Technology, Inc.) and Alexa Fluor 555-conjugated goat anti-rabbit IgG (H+L) (1:500; cat. no. 4413; Cell Signaling Technology, Inc.). Images were acquired using an Olympus fast, high-resolution, inverted fluorescence imaging system (Olympus Corporation).

In each segment on the tissue microarray, five random high-magnification (x400 magnification) fields were analyzed using a bi-rater semi-quantitative assessment method for scoring. The expression of Gab2 was evaluated semi-quantitatively as follows: A score of 0 was given for <5% of cells exhibiting positive staining, 1 for 6-25%, 2 for 26-50%, and 3 for >50%. Concurrently, the staining intensity was graded on a scale of 0 (negative), 1 (faint), 2 (moderate), and 3 (strong). Consequently, the staining index was calculated as the product of the positivity percentage and intensity score, averaged over five fields of view. Accordingly, a total score of 0-4 indicated a low Gab2 expression, and a score of 5-9 indicated a high expression of Gab2.

Mice. BALB/c mice (female, 5-6 weeks old; n=45; weighing 20±1.5 g) were purchased from Chongqing Tengxin Bio-Technology Co., Ltd. The animals were housed under specific pathogen-free conditions in environment with regulated temperature (25±1°C) and humidity (40-70%) and exposure to a constant 12-h light/dark cycle in the animal facility at Zunyi Medical University (Zunyi, China). All animal experiments were performed according to the guidelines for the Care and Use of Laboratory Animals (Ministry of Health, China, 1998). The experimental procedures were approved by the ethical guidelines the Zunyi Medical University Laboratory Animal Care and Use Committee (permit no. 2018016). All experiments were repeated three times.

Cells and cell culture. The human monocytic cell line (THP-1) and BALB/c mouse colon adenocarcinoma cell line (CT26) were obtained from The Cell Bank of Type Culture Collection of the Chinese Academy of Sciences. Fetal human

colonic mucosa cells (FHC) and human CRC cell lines (SW620, SW480 and HCT116) were kept in the Immunology Laboratory of Zunyi Medical University. The THP-1 cells were cultured in RPMI-1640 medium (cat. no. SH30027.01; HyClone; Cytiva) supplemented with 10% fetal bovine serum (FBS; Thermo Fisher Scientific, Inc.), 0.11 g/l sodium pyruvate (cat. no. C0331; Beyotime Institute of Biotecnology) and 1% penicillin-streptomycin (cat. no. P1400; Beijing Solarbio Science & Technology Co., Ltd.) at 37˚C in 5% CO_2. The THP-1 monocytes were differentiated into macrophages with 100 ng/ml phorbol 12-myristate 13-acetate (PMA; cat. no. P1585; MilliporeSigma) for 24 h. The CT26 and HCT116 cells were cultured in high-glucose DMEM (cat. no. SH30243.01; HyClone; Cytiva) supplemented with 10% FBS and 1% penicillin-streptomycin. The SW620 and SW480 cells were cultured in L-15 medium (cat. no. SH30525.01; HyClone; Cytiva) supplemented with 10% FBS and 1% penicillin-streptomycin. For the primary culture of BMDMs, bone marrow cells were harvested from 6-to 8-week-old female BALB/c mice (n=3). In brief, bone marrow cells were isolated from the femur and tibia via fine dissection. Red blood cells were lysed, and the remaining bone marrow cells were cultured in high-glucose DMEM containing 10% FBS and 1% penicillin-streptomycin, supplemented with 20 ng/ml recombinant murine M-CSF (cat. no. 315-02, PeproTech, Inc.) and maintained at 37˚C in 5% CO_2. BMDM were harvested after 7 days of M-CSF-mediated macrophage differentiation. Peritoneal cells were collected from BALB/c mice, briefly, a total of 3 female BALB/c mice were sacrificed, and the skin was removed from the abdominal area. Mice were then injected intraperitoneally with 4-5 ml PBS using a 4.5 gauge needle. Without extracting the needle, the abdomen was gently massaged and then as much fluid from the peritoneum as possible was slowly withdrawn with the syringe. Following removal, the peritoneal cells were gently washed with PBS prior to use, and then seeded at a concentration of $2x10^6$/ml in plates containing RPMI-1640 medium supplemented with 10% FBS and 1% penicillin-streptomycin. The cells were incubated for 12 h at 37˚C in 5% CO_2, and non-adherent cells were then washed out with PBS; the remaining adherent cells were peritoneal macrophages (PMΦ). Polarization of PMΦ towards the M1 phenotype was achieved by stimulation with lipopolysaccharide (LPS; cat. no. L2880-10MG; MilliporeSigma) 100 ng/ml and interferon-γ (IFN-γ; cat. no. 315-05; PeproTech, Inc.) 20 ng/ml for 24 h. On the other hand, polarization towards the M2 phenotype was generated by incubation of macrophages with interleukin-4 (IL-4; cat. no. 214-4; PeproTech, Inc.) 20 ng/ml for 24 h.

Preparation of tumor-conditioned medium (TCM). The CT26 cells were seeded in flasks and cultured in high-glucose DMEM supplemented with 10% FBS and 1% penicillin-streptomycin. Upon reaching a confluency >60%, the medium was replaced with fresh high-glucose DMEM, and incubation was continued for 48 h at 37˚C in 5% CO_2. Subsequently, the supernatant was collected and centrifuged at 12,000 x g for 10 min at 4˚C. A sterile 0.22-μm filter was used to filter the supernatant following centrifugation. The supernatant was then aliquoted and kept at -80˚C for use in further experiments.

Knockdown of Gab2 in PMΦ cells. The lentiviral interference vector (LV-Gab2-shRNA), and the negative control viral vector [CON077 (hU6-MCS-Ubiquitin-EGFP-IRES-puromycin)], were designed, constructed, and packaged by Shanghai Genechem Co., Ltd., with specifics listed in Table SI. The recombinant GV248 lentiviral vector plasmid or the negative control lentiviral vector plasmid and pHelper 1.0 plasmid, the pHelper 2.0 plasmid (Shanghai Genechem Co., Ltd.) were co-transfected into 293T cells (American Type Culture Collection) via HitransG enhanced infection solution (Shanghai Genechem Co., Ltd.) at 37˚C in 5% CO_2 for 6 h. The high-glucose DMEM supplemented with 10% FBS medium was refreshed. The culture supernatants were collected at 48 h following transfection. Following centrifugation at 4,000 x g for 10 min at 4˚C to remove cell debris, the supernatant was filtered through 0.45-μm polyethersulfone low protein-binding filters. The concentrated viral supernatant was aliquoted and kept at -80˚C prior to use. The lentivirus was diluted with serum-free high-glucose DMEM medium, followed by the addition of diluted lentiviral particles and polybrene (final concentration is 8 μg/ml) to PMΦ cells at a multiplicity of infection (MOI) of 80. Following an 8-12 h at 37˚C in 5% CO_2 incubation, the medium was refreshed. Subsequently, at 72 h post-infection, the PMΦ cells were harvested for further analysis, and the transfection efficiency was verified using reverse transcription-quantitative PCR (RT-qPCR) and immunofluorescence.

Establishment of the mouse subcutaneous tumor xenograft model. BALB/c wild-type (WT) female mice (5-6 weeks old; weighing 20±1.5 g) were divided into three groups. In the first group (CT26 group), a total of $2x10^5$ CT26 cells suspended in 100 μl PBS were injected subcutaneously into the left flank of the mice (n=3). In the second group (Gab2^{WT}-CT26), a 100 μl mixture of PMΦ ($2x10^4$) infected with LV-Con and CT26 ($2x10^5$) cells suspension was injected subcutaneously into the left flank of the mice (n=3). In the third group (Gab^{Def}-CT26), a 100 μl mixture of PMΦ infected with LV-Gab2 ($2x10^4$) and CT26 ($2x10^5$) cells suspension was injected subcutaneously into the left flank of the mice (n=3). Tumor size was initially evaluated on the 6th day post-injection using calipers and the length and width of the tumors was then monitored every 2 days, the tumor volume was calculated according to the following formula: (length x width^2)/2. The health and behavior of the animals were monitored every 3 days. No mice succumbed and there were no abnormal signs of humane endpoints over the course of the experiment. Tumor growth curves were plotted for each group of mice based on the measurements. On the 21st day following the implantation of CT26 cells, the mice were sacrificed via cervical dislocation. Death was confirmed by continuing to observe the mice for 3 min after the observation of no heartbeat, respiration and the pupils are dilated, then the tumor tissues were isolated for subsequent analyses. The humane endpoints for the experiment were designated as follows: A marked reduction in food or water intake, labored breathing, an inability to stand and no response to external stimuli. However, no abnormal signs that were indicative of humane endpoints of the experiment were observed in any of the mice during these experiments. All mouse experiments lasted 1 month and included acclimatization to the feeding environment, tumor implantation and growth.

Isolation of macrophages from murine tumor tissue and fluorescence-activated cell sorting. Tumor tissues were extracted from the mice, and the fascia, fat and necrotic zones were cleared. A single-cell suspension of tumor tissue was prepared using the Mouse Tumor Dissociation kit (cat. no. 130-096-730; Miltenyi Biotechnology Co., Ltd.) according to the manufacturer's instructions. The resulting single-cell suspension was resuspended in cold PBS buffer and centrifuged at 300 x g for 7 min at 4˚C. The cell concentration was adjusted to $6x10^5$ per tube, and the F4/80 antibody (0.5 μg/test; cat. no. 11-4801-85; Invitrogen; Thermo Fisher Scientific, Inc.) was added and incubated on ice for 30 min, protected from light. The stained single-cell suspension of tumor tissue were analyzed, and the macrophages were selectively sorted utilizing a Beckman Gallios flow cytometer (Beckman Coulter, Inc.).

Immunofluorescence. The cells on coverslips were fixed in 4% paraformaldehyde for 15 min at 4˚C, blocked with bovine serum albumin (BSA) for 60 min at room temperature, and then incubated overnight at 4˚C with the appropriate primary antibodies. The primary antibodies utilized were as follows: F4/80 (1:200; cat. no. ab6640; Abcam), Gab2 (1:50; cat. no. 22549-1-AP; Proteintech Group, Inc.), CD206/macrophage mannose receptor (CD206; 1:500; cat. no. 18704-1-AP; Proteintech Group, Inc.) and arginase-1 (Arg-1; 1:10,000; cat. no. 16001-1-AP; Proteintech Group, Inc.). Subsequently, the coverslips were rinsed three times with cold PBS for 5 min each time. This was followed by a 2-h incubation at room temperature in the dark with the following secondary antibodies: Alexa Fluor 488-conjugated goat anti-rabbit IgG (H+L) (1:500; cat. no. 4412; Cell Signaling Technology, Inc.) and Alexa Fluor 555-conjugated goat anti-rabbit IgG (H+L) (1:500; cat. no. 4413; Cell Signaling Technology, Inc.). Images were acquired using an Olympus fast, high-resolution, inverted fluorescence imaging system (Olympus Corporation).

RNA extraction and RT-qPCR. Total RNA was isolated from the PMΦ, BMDM, macrophages sorted from subcutaneously transplantated tumors in mice (Tu-TAM) and macrophages cultured in TCM (TCM-TAM) using RNAiso Plus (cat. no. 9108; Takara Biotechnology Co., Ltd.) according to the manufacturer's instructions. A total of 3 μg RNA was reverse transcribed into cDNA using the RT reagent kit (cat. no. RR037A; Takara Biotechnology Co., Ltd.). qPCR was conducted using a Bio-Rad CFX96 detection system (Bio-Rad Laboratories, Inc.) with 25 μl PCR mix containing 12.5 μl SYBR-Green master mix, 2 μl primer mix, 2 μl cDNA and 8.5 μl deionized water. The RT-qPCR thermocycling conditions were as follows: Initial denaturation at 95˚C for 30 sec, followed by 40 cycles at 95˚C for 5 sec and 60˚C for 30 sec. The relative mRNA expression levels of genes were calculated using the comparative threshold cycle ($2^{-\Delta\Delta Cq}$) method (28), utilizing GAPDH as the reference gene. All primers were synthesized by Sangon Biotech (Shanghai) Co., Ltd., and are listed in Table SII.

Protein extraction and western blot analysis. Proteins were extracted from the PMΦ, BMDM, THP-1, Tu-TAM, TCM-TAM using cell lysis buffer (cat. no. 9803; Cell Signaling Technology, Inc.), followed by centrifugation at 12,000 x g for 10 min at 4˚C. The protein concentration was quantified using the BCA Protein Quantitation kit (cat. no. GK5011; Shanghai Generay Biological Engineering Co., Ltd.). A total of 30 μg protein per well was loaded and electrophoresed on a 10% SDS-PAGE gel to achieve protein separation based on molecular weights. The proteins were then transferred onto PVDF membranes (cat. no. IPVH00010; Merck Millipore). The membranes were blocked with 5% skim milk at room temperature for 2 h and then incubated with specific primary antibodies overnight at 4˚C. The primary antibodies used were as follows: Gab2 (1:1,000; cat. no. 22549-1-AP; Proteintech Group, Inc.), CD206 (1:500; cat. no. 18704-1-AP; Proteintech Group, Inc.), Arg-1 (1:10,000; cat. no. 16001-1-AP; Proteintech Group, Inc.), ERK1/2 (1:1,000; cat. no. 4695; Proteintech Group, Inc.), phosphorylated (p-)p44/42 MAPK (ERK1/2) (Thr202/Tyr204; 1:1,000; cat. no. 9101 Proteintech Group, Inc.), AKT (1:1,000; cat. no. 9272; Proteintech Group, Inc.), p-AKT (Ser473; 1:1,000; cat. no. 4058; Proteintech Group, Inc.), signal transducer and activator of transcription (STAT)3 (1:1,000; cat. no. 9132; Proteintech Group, Inc.), p-STAT3 (Tyr705; 1:1,000; cat. no. 9131; Proteintech Group, Inc.), STAT6 (1:1,000; cat. no. ab32520; Abcam), p-STAT6 (Y641; 1:1,000; cat. no. ab263947; Abcam), GAPDH (1:1,000; cat. no. 2118; Proteintech Group, Inc.) and then incubated with goat anti-rabbit IgG (H+L)-HRP [1:5,000; cat. no. abs20147; Aibixin (Shanghai) Biotechnology Co., Ltd.] for 2 h at room temperature. The proteins were visualized by enhanced chemiluminescence using the ECL assay kit (cat. no. WBKLS0100; Merck Millipore). ImageJ software (version 1.8.0; National Institutes of Health) was used to quantify the protein band intensities.

Hematoxylin and eosin (H&E) staining. Tumor and lung tissues from the mice in the xenograft tumor model were subjected to paraffin embedding, sectioning and H&E staining with the assistance of the Department of Pathology, Affiliated Hospital of Zunyi Medical University. Briefly, the tumor and lung tissues were fixed in 10% neutral formalin for 48 h at room temperature, embedded in paraffin, and sectioned at a thickness of 3 μm. This was followed by deparaffinization and rehydration using a series of laboratory graded alcohol at different percentages (75%; 85%; 95%-I; 95%-II; 95% alcohol-III, dimethyl benzene-I and dimethyl benzene-II). Alcohol and dimethyl benzene were obtained from Guizhou Keode Biotechnology Co., Ltd., respectively and the sections were stained with hematoxylin for 8 min and eosin solution for 40 sec at room temperature (G1120; Beijing Solarbio Science & Technology Co., Ltd.), and the tissue sections were rinsed under running water. Finally, the tumor and lung tissues structures were observed under a full slide scanning microscope (Olympus Corporation).

Statistical analysis. Statistical analyses were conducted using IBM SPSS 21 and GraphPad Prism 7 software. The experimental results are presented as the mean standard deviation (mean ± SD). A two-tailed unpaired Student's t-test was used to compare two datasets. For multiple group comparisons, one-way ANOVA followed by Tukey's post hoc test was used. The Chi-squared test was used for the evaluation of categorical data. Survival curves were illustrated using Kaplan-Meier plots and analyzed using the log-rank test. Univariate and multivariate

Carcinoma tissues (1, 3, 5, ...17): 93 patients; Paracancerous tissues (2, 4, 6 ...18): 87 patients.
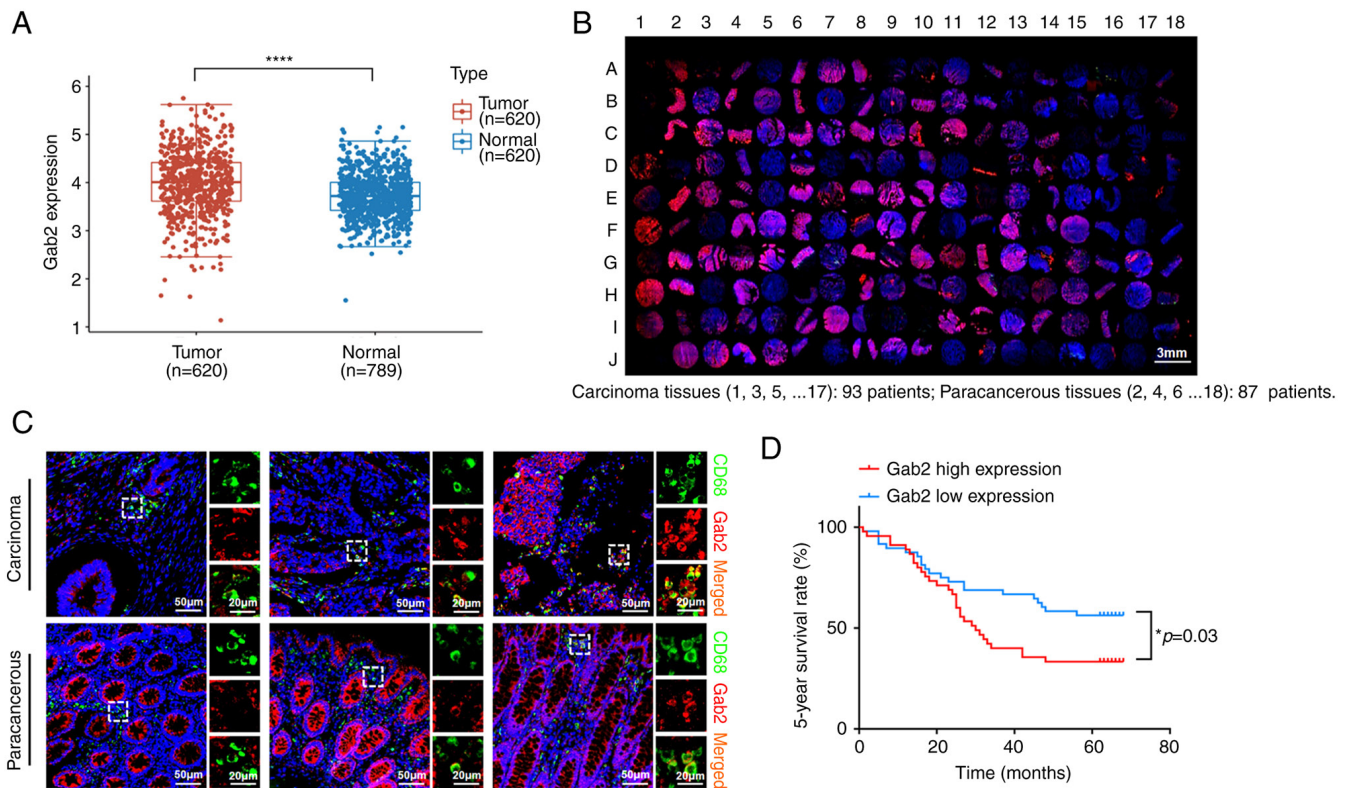
Figure 1. Gab2 is upregulated within TAMs in tumor tissues and is associated with the poor prognosis of patients with CRC. (A) Expression level of Gab2 in CRC and adjacent normal tissues from The Cancer Genome Atlas database. ****$P < 0.0001$, tumor vs. normal. (B) Representative images of immunohistochemical staining of Gab2 and CD68 in colorectal carcinoma and para-cancerous tissues. (C) Multiplex immunofluorescence staining of the macrophage markers, CD68 and Gab2. CD68 staining is shown in green, Gab2 is shown in red, and DAPI staining in blue. The panels on the right of each image are enlarged images of the boxed area in the main images. (D) The association between Gab2 expression in TAMs and the 5-year survival rate of patients with CRC. According to the median of the immunofluorescence intensity score, the patients with CRC were divided into two groups (Gab2 low expression and Gab2 high expression). Survival curves were plotted using the Kaplan-Meier method, and the statistical significance of the difference in 5-year survival rates between the groups was assessed using the log-rank test. *$P < 0.05$. Gab2, Gab2, Grb2-associated binder 2; TAMs, tumor-associated macrophages; CRC, colorectal cancer.

Cox regression analysis was used to analyze the factors affecting the 5-year survival rates of patients with CRC. $P < 0.05$ was considered to indicate a statistically significant difference.

Results

Gab2 is upregulated within TAMs in tumor tissues and is associated with a poor prognosis of patients with CRC. Firstly, the present study analyzed the mRNA expression of Gab2 using publicly accessible datasets from The Cancer Genome Atlas (TCGA). The analysis revealed a significant elevation in Gab2 mRNA expression in the CRC tumor tissues compared to the normal tissues (Fig. 1A). To identify the role of Gab2 in TAMs, the expression levels of Gab2 and CD68 in the CRC tissue array were evaluated using immunofluorescence staining (Fig. 1B). The results indicated that Gab2 was predominantly localized in the cytoplasm of TAMs, with a nuclear localization rarely observed; an elevated expression of Gab2 was found within TAMs in the tumor tissues compared to TAMs in para-cancerous tissue (Fig. 1C and Table I). Subsequently, the patients with CRC were categorized into two groups based on the median expression level of Gab2 immunofluorescence intensity: A high and low Gab2 expression within TAMs. Upon further analysis, no significant differences were found between the two groups as regards conventional prognostic factors, including sex, age, degree of histological differentiation,

tumor volume size, TNM stage and clinical stage (Table II). Notably, the findings indicated that an elevated expression of Gab2 within TAMs was associated with a poor 5-year survival rate of patients with CRC (Fig. 1D). Using univariate and multivariate COX regression analyses, it was revealed that the expression level of Gab2 within TAMs was a potentially pivotal factor influencing the 5-year survival rate of patients with CRC (Table III).

TAMs in tumor tissues exhibit a higher expression of Gab2 and the M2 phenotype. To elucidate the role of Gab2 within TAMs, its expression in TAMs was initially investigated using TCM from various tumor cell lines to culture macrophages to simulate the TME. Firstly, PMΦ (Fig. 2A-D) and BMDM (Fig. 2E and F) were cultured with a TCM from CT26 cells for 24 h to verify Gab2 expression within TAMs. Furthermore, TCM derived from FHC cells and human CRC cell lines, including HCT116, SW480 and SW620 cells, was used to culture with PMA-differentiated human THP-1 monocytes to evaluate Gab2 expression within TAMs (Fig. 2G). Cumulatively, the results revealed a significantly elevated Gab2 expression within the TCM-TAMs compared to the normal macrophages or macrophages that were cultured with TCM from the FHC cell line. To further verify the expression of Gab2 within TAMs *in vivo*, a subcutaneously transplanted tumor model was established using CT26 cells. On the 21st day

Table I. Expression of Gab2 in TAMs from colorectal carcinoma and para-cancerous tissues.

| Group | No. of patients | Gab2 expression | | | P-value |
		Positive	Negative	Positive rate	
Colorectal carcinoma	93	70	23	75.3%	P<0.05
Para-cancerous	87	37	50	42.5%	

Gab2, Grb2-associated binder 2; TAMs, tumor-associated macrophages.

Table II. Gab2 expression and clinicopathological characteristics of patients with CRC.

| | Patient group (n=93) | | | | | |
| | Gab2 low expression (n=48) | | Gab2 high expression (n=45) | | | |
Variable	No. of patients	%	No. of patients	%	Chi-squared test	P-value
Sex					0.1229	0.7529
Male	26	54.2	26	57.8		
Female	22	45.8	19	42.2		
Age, years					2.3911	0.122
<60	12	25.0	18	40.0		
≥60	36	75.0	27	60.0		
Tumor volume (cm^3)					0.2726	0.6016
<14	25	52.1	21	46.7		
>14	23	47.9	24	53.3		
Differentiation					0.4593	0.489
I-II, II	40	83.3	35	77.8		
II-III, III	8	16.7	10	22.2		
T stage					1.1042	0.5757
T2	2	4.2	3	6.7		
T3	36	75	36	80		
T4	10	20.8	6	13.3		
N stage					0.8009	0.67
N0	31	64.6	25	55.6		
N1	13	27.1	25	33.3		
N2	4	8.3	5	11.1		
M stage					0.0044	0.9474
M0	46	95.8	43	95.6		
M1	2	4.2	2	4.4		
Clinical stage					1.5523	0.6703
I	1	2.1	3	6.7		
II	26	54.2	20	44.4		
III	19	39.6	20	44.4		
IV	2	4.2	2	4.4		

Gab2, Grb2-associated binder 2; CRC, colorectal cancer.

post-injection, tumor tissues were harvested, and single-cell suspensions were prepared to analyze and isolate TAMs for further investigation. It was observed that the proportion of TAMs was ~7.7% (Fig. 2H). Notably, a significantly heightened expression of Gab2 was observed within Tu-TAM compared to PMΦ isolated from tumor-free mice (Fig. 2I and J). In

Table III. Univariate and multivariate analysis of survival-related factors of patients with CRC.

Variable	Univariate analysis			Multivariate analysis		
	HR	95% CI	P-value	HR	95% CI	P-value
Gab2 (high vs. low)	1.858	1.061-3.255	0.03	1.936	1.077-3.483	**0.027**
Age/years (≥60 vs. <60)	1.105	0.597-2.046	0.750	1.627	0.841-3.149	0.148
Tumor volume (cm^3) (≥14 vs. <14)	2.073	1.173-3.662	0.012	1.936	1.078-3.474	**0.027**
TNM stage (III-IV vs. I-II)	3.263	1.845-5.771	0.001	4.011	1.597-10.075	**0.003**
Lymph node metastasis (yes vs. no)	2.328	1.337-4.063	0.003	0.741	0.307-1.790	0.506
Distant metastasis (yes vs. no)	2.382	0.850-6.672	0.099	1.288	0.435-3.813	0.648

Values in bold font indicate statistically significant differences (P<0.05). Gab2, Grb2-associated binder 2; CRC, colorectal cancer.
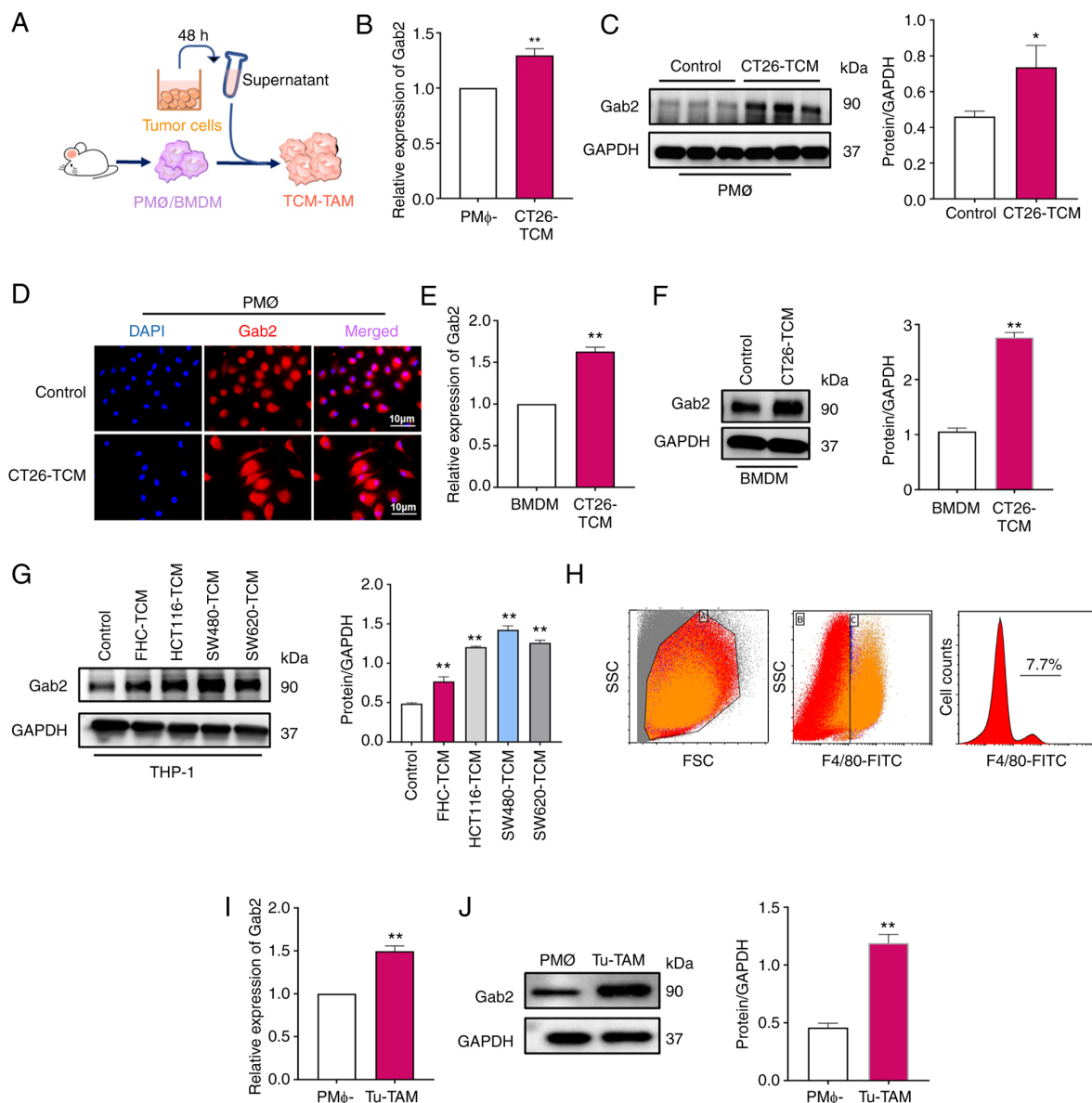

Figure 2. TAMs in tumor tissues exhibit a higher expression of Gab2 and the M2 phenotype. (A) Diagram of the simulated tumor microenvironment *in vitro*. (B-D) Gab2 expression levels in TCM-stimulated PMΦ. (E and F) Gab2 expression levels in TCM-stimulated BMDM. (G) Gab2 expression in TCM-stimulated THP-1 cells. (H) The expression of Gab2 in TAMs harvested from CT26 tumor-bearing mice and the percentage of macrophages was analyzed using fluorescence-activated cell sorting. (I) The *Gab2* mRNA expression levels in Tu-TAM were measured using reverse transcription-quantitative PCR. (J) The protein expression of Gab2 in Tu-TAM was detected using western blot analysis. **P<0.01, Tu-TAM vs. PMΦ. TAMs, tumor-associated macrophages; Gab2, Gab2, Grb2-associated binder 2; TCM, tumor-conditioned medium; PMΦ, peritoneal macrophages; BMDM, bone marrow-derived macrophages; Tu-TAM, macrophages sorted from subcutaneously transplanted tumors in mice.

summary, these results highlight the elevated expression of Gab2 within TAMs both *in vitro* and *in vivo*, suggesting its potential role in regulating TAMs.

To determine the polarization phenotype of TAMs, PMΦ were used as M0 macrophages, which were further polarized into M1 macrophages using LPS and IFN-γ stimulation, or into M2 macrophages using IL-4 stimulation, thereby representing the two opposite states of macrophage polarization. Subsequently, the mRNA expression of M1 markers [inducible nitric oxide synthase (*Inos/Nos2*), *Il-12* and C-X-C motif chemokine ligand 9 (*Cxcl9*)] and M2 markers [*Il-10*), *Arg-1*, chitinase-like protein 3 (*Ym-1/Chil3*), resistin-like molecule alpha (*Fizz1/Retnla*), C-C motif chemokine ligand 17 (*Ccl17*) and vascular endothelial growth factor (*Vegf*)] in PMΦ, Tu-TAM, TCM-TAM was analyzed using RT-qPCR. The results revealed the significant suppression of the M1 markers, *Inos* and *Il-12*, in Tu-TAM and TCM-TAM compared to PMΦ (Fig. 3A). By contrast, a marked elevation of M2 marker expression was observed in Tu-TAM, TCM-TAM compared to PMΦ (Fig. 3B). Furthermore, the results of western blot analysis revealed that the expression of M2 macrophage markers (CD206 and Arg-1) was significantly upregulated in the Tu-TAM and TCM-TAM (Fig. 3C). Taken together, these results indicated that TAMs exhibit an M2-like phenotype.

Silencing of Gab2 expression impedes the M2 polarization of TAMs. To further investigate the effects of Gab2 on TAM polarization, PMΦ were infected with LV-CON and three Gab2 lentiviral interference vectors (LV-Gab2-sh1, LV-Gab2-sh2 and LV-Gab2-sh3). The transfection efficiency was examined using RT-qPCR and immunofluorescence staining. It was observed that transfection at an MOI of 80 achieved >80% infection efficiency while simultaneously maintaining the normal cell confluence and showing no signs of unusual morphological changes (Fig. 4A). The analyses revealed that among the three shRNAs, LV-Gab2-sh3 effectively suppressed Gab2 expression in PMΦ (Fig. 4B and C). Consequently, LV-Gab2-sh3 was selected for use in subsequent experiments. LV-Gab2-sh3 was used to suppress Gab2 expression in PMΦ; these cells were then incubated with TCM for 24 h to investigate the expression of TAM polarization-related molecules. The results demonstrated that the suppression of Gab2 expression in PMΦ significantly decreased the mRNA levels of M2 macrophage markers compared to the LV-CON control group. Furthermore, it was evident that the mRNA levels of TCM-induced M2-associated molecules, including *Il-10*, *Arg-1*, *Ym-1*, *Fizz1*, *Ccl17* and *Vegf* were significantly reduced in the cells in which Gab2 expression was suppressed (Fig. 4E). However, the expression levels of M1 markers, such as *Inos*, were increased, whereas *Il-12* and *Cxcl9* remained relatively unaltered (Fig. 4D). As was expected, the results of western blot analysis confirmed that the suppression of Gab2 expression significantly led to a notable reduction in the expression of M2-associated molecules, such as CD206 and Arg-1 (Fig. 4F). Taken together, these data indicate that the downregulation of Gab2 expression serves as a significant barrier to the M2 polarization of TAMs.

Suppression of Gab2 expression reduces TAM-mediated CRC tumorigenesis. To explore the role of Gab2 in modulating

TAM polarization and its effects on CRC progression, a CRC xenograft mouse model was established using CT26 cells, Gab^{WT}-CT26 cells and Gab2^{Def}-CT26 cells subcutaneously injected into the left flanks of mice. On the 21st day post-injection, the mice were euthanized, and tumor tissues were dissected and weighed (Fig. 5A and B). Notably, the Gab2^{Def}-CT26 group demonstrated a significant inhibition in subcutaneous tumor progression, displaying a marked reduction in tumor volume compared to the CT26 and Gab2^{WT}-CT26 groups. Specifically, the Gab2^{WT}-CT26 group exhibited significant increases in both tumor volume and weight (Fig. 5C and D). Histological analyses revealed that the Gab2^{Def}-CT26 group exhibited a reduction in abnormal enlargement and hyperchromatism in the tumor nuclei. Additionally, there was a significant decrease in the population of heteromorphic cells in the tumor tissue, along with the most reduced infiltration of metastatic tumor cells within the lung tissue compared to CT26 and Gab2^{WT}-CT26 groups (Fig. 5E). Furthermore, immunofluorescence analysis demonstrated that the expression of Gab2, CD206 and Arg-1 within TAMs in the tumor tissues was markedly reduced in the Gab2^{Def}-CT26 group, compared to the CT26 and Gab^{WT}-CT26 groups (Fig. 5F). Collectively, these observations underscore that Gab2 plays a pro-tumorigenic role in CRC, establishing that its suppression can effectively reduce the TAM-mediated promotion of CRC tumorigenesis.

Gab2 induces M2-like macrophage polarization through the AKT/ERK signaling pathway. The results indicated that the suppression of Gab2 expression impedes TAM polarization into M2-like macrophages, consequently inhibiting CRC growth in mice. Adams *et al* (29) demonstrated that Gab2 was essential for two major signal transduction pathways in cancer, namely the PI3K-AKT and ERK signaling pathways, orchestrating numerous key cellular processes. Therefore, the present study evaluated the protein expression and phosphorylation levels of AKT, ERK1/2, STAT3 and STAT6 in signaling pathways associated with macrophage polarization using western blot analysis. The results revealed significantly increased levels of p-AKT and p-ERK1/2 in the TCM-LV-Con compared with the LV-Con group. Conversely, the TCM-LV-Gab2 group exhibited notably decreased levels of p-AKT and p-ERK1/2 compared to the TCM-LV-Con group, while no significant variations were observed in the levels of p-STAT6 and p-STAT3 (Fig. 6B). On the whole, these findings indicate that the suppression of Gab2 expression significantly hinders the transition of TAMs into an M2-like macrophage state, and culminates in altered phosphorylation levels of key signaling molecules AKT and ERK1/2, serving as a promising target for the treatment of CRC.

Discussion

The pivotal role of Gab2, a molecule associated with tumor growth, progression and metastasis (29,18), has been highlighted in recent studies examining its dysregulated expression across several human cancers, including BRCA (21), OV (22,23), HCC (24,25), CRC (26) and melanoma (27), as well as its potential as a novel oncogene. A previous study by the authors demonstrated a high expression of Gab2 in CRC tissues and cell lines, particularly in specimens from patients
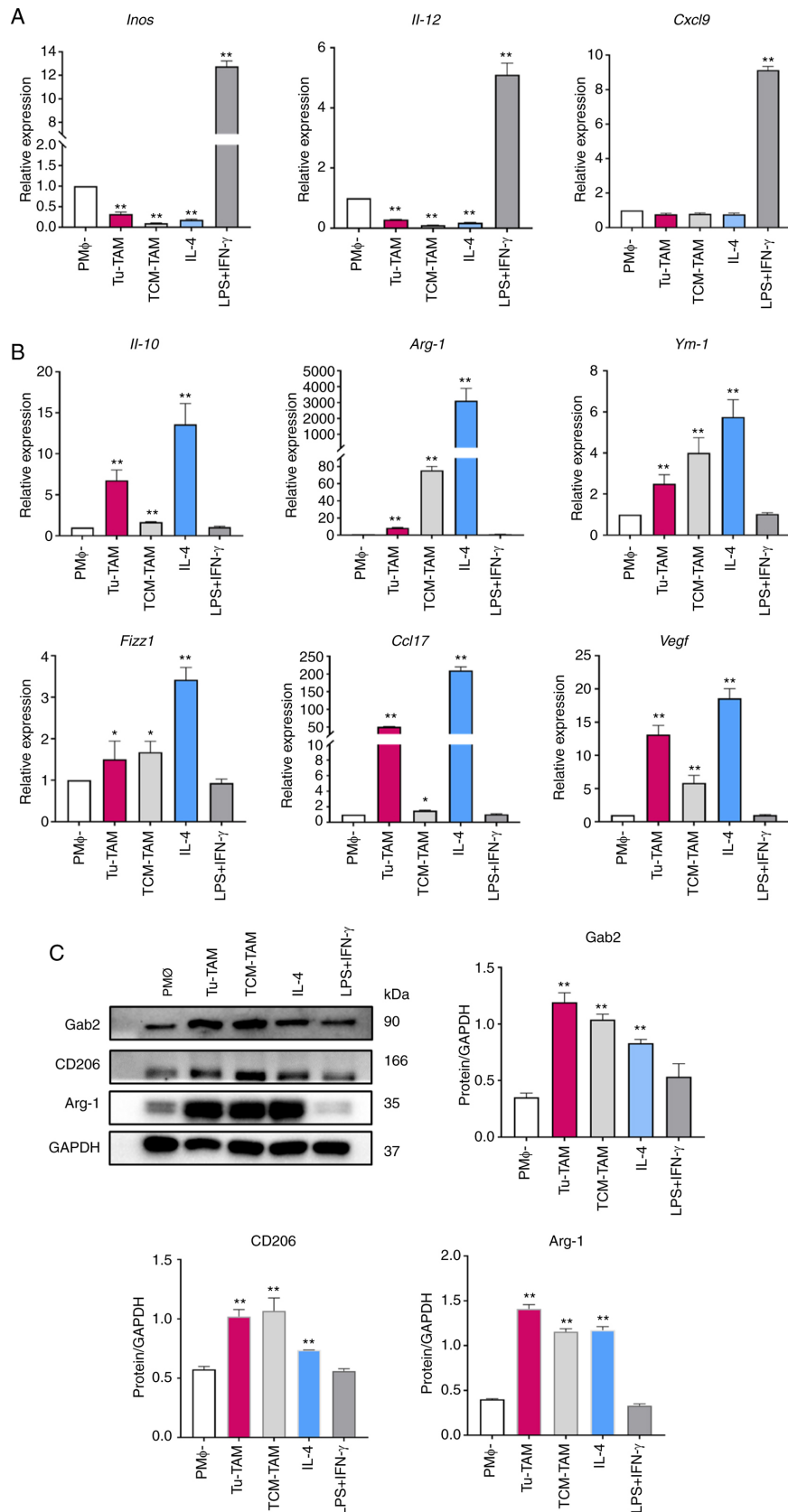
Figure 3. Expression of TAM polarization-related molecules. PMΦ from BALB/c mice were stimulated with LPS + IFN-γ and IL-4 for 24 h, serving as an M1/M2 positive control. (A) Evaluation of *Inos*, *Il-12* and *Cxcl9* mRNA expression levels in PMΦ, Tu-TAM, TCM-TAM using RT-qPCR. **P<0.01, Tu-TAM, TCM-TAM, IL-4, LPS + IFN-γ vs. PMΦ. (B) Evaluation of *Il-10*, *Arg-1*, *Ym-1*, *Fizz1*, *Ccl17*, *Vegf* mRNA expression levels in PMΦ, Tu-TAM, TCM-TAM using RT-qPCR. *P<0.05, Tu-TAM, TCM-TAM vs. PMΦ. **P<0.01, Tu-TAM, TCM-TAM, IL-4 vs. PMΦ. (C) Evaluation of Arg-1, CD206 protein levels in PMΦ, Tu-TAM, TCM-TAM using western blot analysis. **P<0.01, Tu-TAM, TCM-TAM, IL-4 vs. PMΦ. TAMs, tumor-associated macrophages; PMΦ, peritoneal macrophages; LPS, LPS, lipopolysaccharide; IFN-γ, interferon-γ; IL, interleukin; *Inos*, inducible nitric oxide synthase; *Cxcl9*, C-X-C motif chemokine ligand 9; Tu-TAM, macrophages sorted from subcutaneously transplanted tumors in mice; TCM, tumor-conditioned medium; RT-qPCR, reverse transcription-quantitative PCR; *Arg-1*, arginase-1; *Ym-1*, Chil3/chitinase-like protein 3; *Fizz1*, Retnla/resistin-like molecule alpha; *Vegf*, vascular endothelial growth factor; *Ccl17*, C-C motif chemokine ligand 17; Gab2, Gab2, Grb2-associated binder 2.
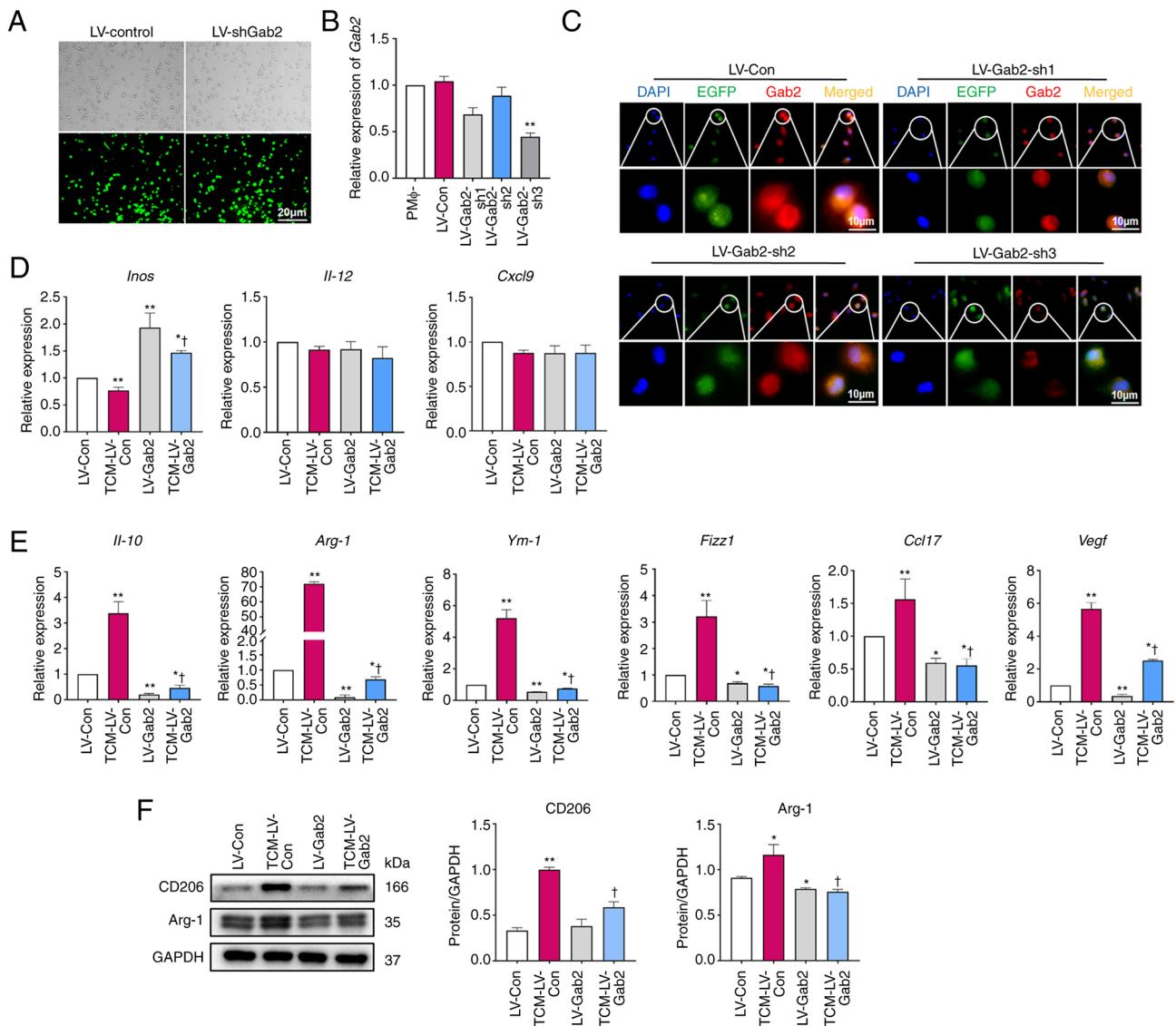
Figure 4. Suppression of Gab2 expression impedes the M2 polarization of TAMs. (A) Visualization of EGFP expression in PMΦ following lentivirus infection. Scale bar, 50 µm. (B and C) The expression of Gab2 in PMΦ post-lentivirus infection. Scar bar, 10 µm. **P<0.01, LV-Gab2 vs. respective control (D) Effect of the suppression of Gab2 expression on the molecules related to TAM M1 polarization. *P<0.05, TCM-LV-Con vs. LV-Con. **P<0.01, LV-Gab2 vs. LV-Con. †P<0.05, TCM-LV-Gab2 vs. TCM-LV-Con. (E) Effect of the suppression of Gab2 expression on TAM M2 polarization markers. *P<0.05, LV-Gab2 vs. LV-Con. **P<0.01, TCM-LV-Con, LV-Gab2 vs. PMΦ. †P<0.05, TCM-LV-Gab2 vs. TCM-LV-Con. (F) Effect of the suppression of Gab2 expression on TAM M2 polarization markers. *P<0.05, TCM-LV-Con, LV-Gab2 vs. LV-Con. **P<0.01, TCM-LV-Con vs. PMΦ. †P<0.05, TCM-LV-Gab2 vs. LV-Con. Gab2, Gab2, Grb2-associated binder 2; TAMs, tumor-associated macrophages; PMΦ, peritoneal macrophages; IL, interleukin; *Arg-1*, arginase-1; *Ym-1*, Chil3/chitinase-like protein 3; *Fizz1*, Retnla/resistin-like molecule alpha; *Vegf*, vascular endothelial growth factor; *Ccl17*, C-C motif chemokine ligand 17.

with CRC with metastases (26). It has also been found that the upregulated expression of Gab2 promotes the proliferation, invasion and metastasis of CRC, indicating its crucial role in the occurrence and development of CRC; this underscores the prospective value of Gab2 as a prognostic predictor for patients with CRC (30,31). TAMs are closely related to the occurrence and development of CRC, notably through polarization transitions that are critical for maintaining the homeostasis of TME (32). Guo *et al* (33) revealed that Gab2 participated in the IL-4-induced M2-like macrophage polarization in bleomycin-induced fibrotic lungs. However, the role of Gab2 in regulating TAM polarization remains largely unexplored. Therefore, an in-depth study of the Gab2 regulation of TAM polarization could uncover Gab2 as a promising predictive biomarker and a feasible therapeutic target for CRC.

The present study reports a novel biological role of Gab2, emphasizing its critical involvement in promoting the alternative activation of TAMs, and thereby promoting CRC growth. The findings presented herein revealed that a high Gab2 expression within TAMs was associated with diminished 5-year survival rates of patients with CRC, indicating the potential effects of Gab2 on the long-term prognosis of patients with CRC. Notably, Cox analysis suggested the Gab2 expression levels in TAMs as a potential pivotal factor in affecting the 5-year survival rate of patients with CRC. However, it did not reveal any significant association between an elevated expression of Gab2 in TAMs and conventional prognostic factors, such as sex, age, the degree of histological differentiation, tumor volume size, TNM stage and clinical stage. This lack of an association calls for more in-depth investigations, urging
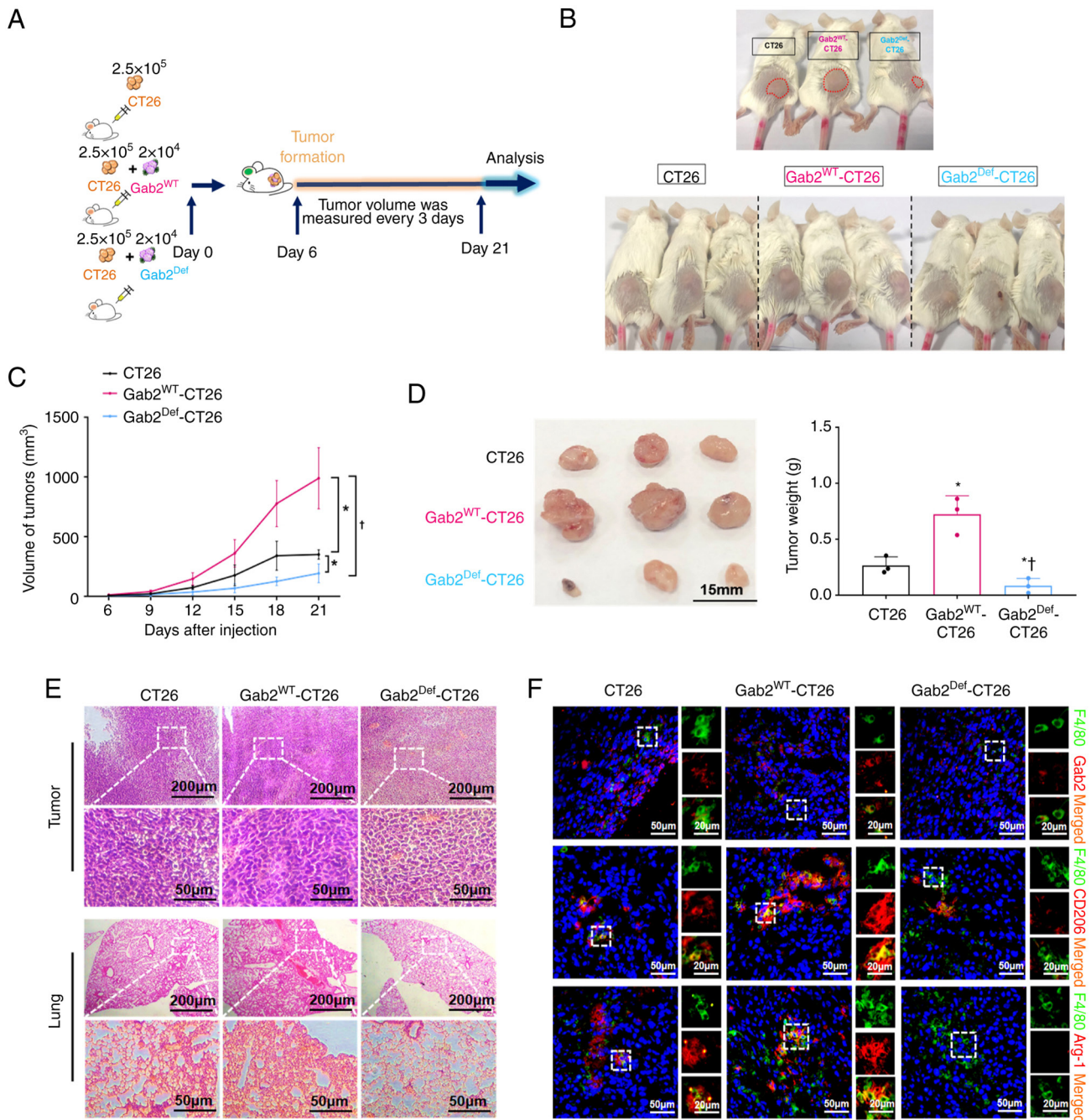
Figure 5. Suppression of Gab2 expression attenuates TAM-mediated CRC tumorigenesis. (A) Diagram of subcutaneous xenograft model. (B) Tumorigenesis assay of BALB/c mice subcutaneously injected with CT26 cells (n=3), Gab2^WT-CT26 cells (n=3) and Gab2^Def-CT26 cells (n=3). (C) Tumor growth curve of the CT26, Gab2^WT-CT26 and Gab2^Def-CT26 groups. (D) Representative photos of harvested tumors from the different experimental groups (left). Scar bar, 15 mm, and the corresponding tumor weight (right). *P<0.05, Gab2^WT-CT26 group vs. CT26 group; †P<0.05, Gab2^Def-CT26 group vs. Gab2^WT-CT26 group. (E) Histopathological analysis of tumor and lung tissues visualized using hematoxylin and eosin staining. (F) Immunofluorescence was performed to detect the expression of Gab2 and M2 polarization markers CD206 and Arg-1 in tumor tissue TAMs. The panels on the right of each image are enlarged images of the boxed area in the main images. Gab2, Grb2-associated binder 2; TAMs, tumor-associated macrophages; Arg-1, arginase-1.

for a comprehensive exploration of the complex network of prognostic factors in CRC. The inconsistencies observed in the present study suggest at the existence of more detailed interactions that govern the outcomes of patients with CRC, which may include factors beyond the traditional prognostic indicators. This presents an opportunity to further examine the intricate association between Gab2 expression and other unknown variables that may significantly influence the survival outcomes of patients with CRC.

The use of a TCM is a pivotal aspect of the experimental approach used herein, as it serves to replicate the intricate TME in the *in vitro* experiments. TCM, enriched with various cytokines, growth factors and other signaling molecules secreted by tumor cells, facilitates the simulation of the complex interactions occurring in the TME. This simulated environment enabled the study of the crucial role of Gab2 in TAMs, providing a more realistic representation of the *in vivo* conditions. To further investigate the role of Gab2 within TAMs, the
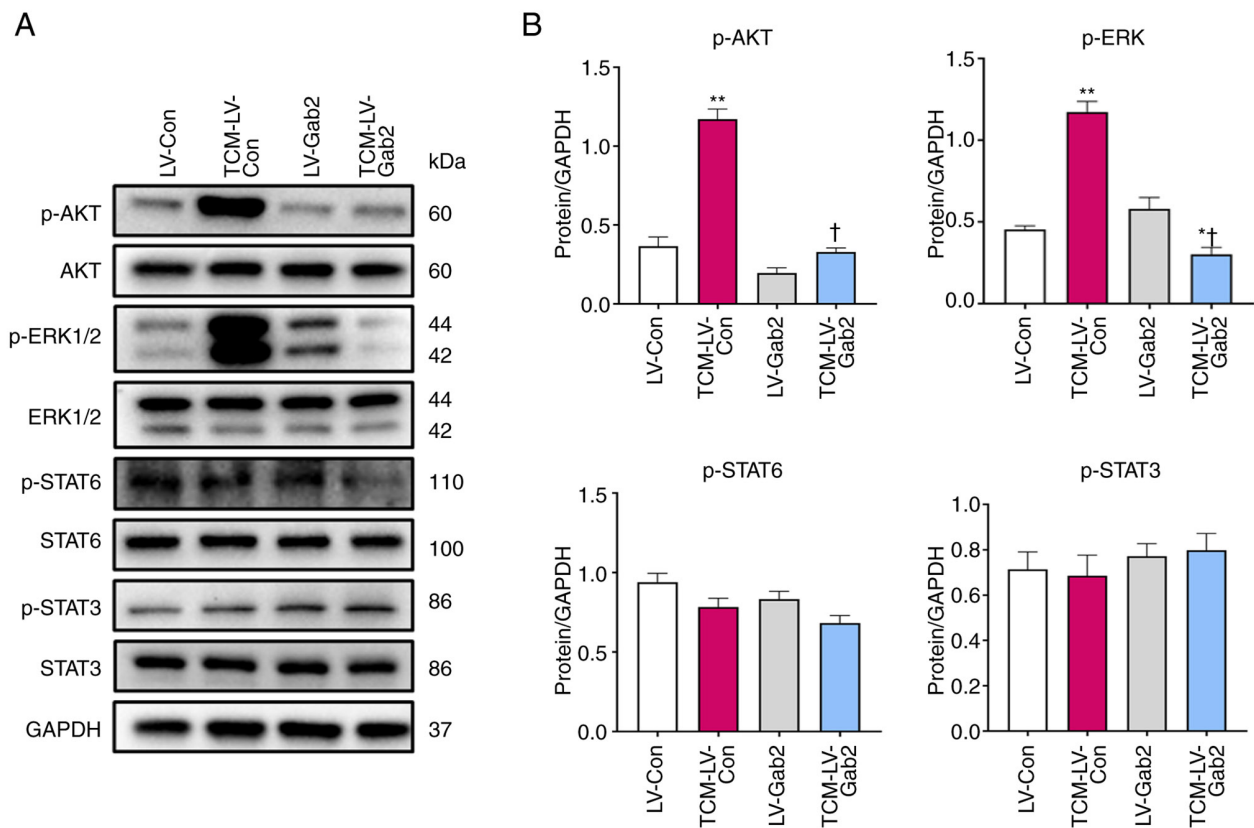
Figure 6. Gab2 induces M2-like macrophage polarization through the AKT/ERK signaling pathway. (A) The expression levels of p-AKT, p-ERK, p-STAT6 and p-STAT3 were measured using western blot analysis. (B) Quantitative evaluation of the expression levels of p-AKT, p-ERK, p-STAT6, p-STAT3. $^{**}P<0.01$, TCM-LV-Con vs. LV-Con. $^{†}P<0.05$, TCM-LV-Gab2 vs. TCM-LV-Con. Grb2-associated binder 2; TCM, tumor-conditioned medium; STAT, signal transducer and activator of transcription.

present study examined its expression in TAMs using TCM from various tumor cell lines to culture macrophages to mimic the TME. The results revealed an elevated expression of Gab2 in TCM-TAMs compared to normal macrophages. It was noted that the majority of TAMs exhibit an M2-like macrophage phenotype, a feature associated with poor outcomes of patients with CRC (34). In the TME, macrophage polarization within tumor tissues is regulated by various signals derived from tumor cells. Influenced by these cytokine signals, TAMs undergo a transition into the M1 and M2 phenotypes (9,35). M1-like macrophages are characterized by the secretion of pro-inflammatory cytokines and have a potent tumor-killing capacity (36). Conversely, M2-like macrophages express immune-related factors, including CD206, Arg-1, Ym-1, Fizz1, IL-10, IL-13, TGF-β, VEGF, matrix metalloproteinases (MMPs), promoting tumor progression and immunosuppression (37-39). The findings of the present study established that TAMs in CRC display characteristics similar to M2-type macrophages and that the suppression of Gab2 expression resulted in decreased M2-associated molecules, consequently inhibiting the M2 polarization of TAMs.

The main causes of the mortality of patients with CRC are post-operative recurrence and distant organ metastasis, with the liver and lungs being the principal metastatic sites (40). Compared with liver metastasis, patients with lung metastasis exhibit a less favorable treatment response, resulting in poorer prognosis and shortened survival periods (41). Consequently, tumor invasion and metastasis significantly diminish the

survival duration and impede the quality of life of patients with CRC (42). In the present study, using a murine model of CRC, it was confirmed that the suppression of Gab2 inhibited TAM-mediated CRC tumorigenesis. Specifically, the Gab2^{Def}-CT26 group exhibited significant tumor growth inhibition, evidenced by a substantial decrease in tumor size, alongside a noticeable reduction in abnormal enlargement and hyperchromatism in the tumor nuclei. Additionally, there was a significant decrease in the population of heteromorphic cells in the tumor tissue, along with the most reduced infiltration of metastatic tumor cells within the lung tissue compared to the CT26 and Gab2^{WT}-CT26 groups. Hence, these results verified the pro-tumorigenic role of Gab2, demonstrating that the suppression of its expression within TAMs inhibits TAM-mediated CRC tumorigenesis.

In eukaryotic cells, multiple signaling pathways, such as the AKT and ERK pathways, are interconnected through complex networks to regulate various cellular processes, including gene expression, cell survival, apoptosis and cell differentiation (43,44). Gab2 functions as an adaptor protein orchestrating several intracellular signaling pathways, acting as a key facilitator of the PI3K/AKT and SHP2/ERK pathways, which regulate tumor cell growth, differentiation, migration and apoptosis (29). Specifically, the authors previously demonstrated that Gab2 facilitated epithelial-to-mesenchymal-transition and CRC metastasis through the activation of the mitogen-activated protein kinase (MEK)/ERK/MMP signaling pathway and promoted CRC

growth and vascularization through the upregulation of VEGF expression mediated by the ERK/c-Myc signaling pathway (30,31). Furthermore, Cheng *et al* (45) found that the inhibition of PI3K, MEK or Jak2 significantly inhibited the Gab2-mediated proliferation and migration of HepG2 cells. Horst *et al* (27) found that Gab2 promoted melanoma cell migration and invasion by activating AKT signaling and enhancing melanoma growth and metastasis *in vivo*. Wang *et al* (46) confirmed that Gab2 overexpression promoted migration and invasion through activation of the PI3K pathway, and inhibited E-calmodulin expression in OV cells. Gong *et al* (19) demonstrated that Gab2 promoted acute myeloid leukemia growth and migration through the SHP2/ERK/CREB signaling pathway. There is evidence to suggest that Gab2 is a central player in engaging various signaling pathways across different types of cancers (30). The present study demonstrated that Gab2 regulates TAM polarization by upregulating the expression of p-AKT and p-ERK.

In conclusion, the present study demonstrated the pivotal role of Gab2 in regulating TAM polarization, providing further insight into the development of immunotherapeutic strategies targeting TAMs. Despite the promising findings, the present study is not without limitations. The emergence of various drugs and inhibitors to modulate TAM polarization is notable. Here are a certain strategies that the authors are considering for future studies, such as: i) Utilizing a Cre-loxP system to conditionally downregulate Gab2 expression specifically in macrophages, allowing for the precise evaluation of the functional consequences of the suppression of Gab2 expression on TAM polarization and CRC progression; ii) exploring the possibility of developing Gab2-specific small molecule antagonists, which can be directed to tumors to bi-directionally regulate CRC cells and macrophages, thereby affecting tumor growth and metastasis; iii) using antisense oligonucleotides designed to specifically bind to Gab2 mRNA, preventing its translation into the protein. These strategies, alone or in combination with other therapeutic treatments, could improve the development of novel clinical therapies targeting Gab2 in CRC, aiming to lay the groundwork for novel antitumor therapeutics.

Availability of data and materials

The datasets used and/or analyzed during the current study are available from the corresponding author upon reasonable request.

Authors' contributions

XG and RL performed the experiments, analyzed the data and wrote the manuscript. MQ performed the experiments and analyzed the data. WZ participated in writing and reviewing the original manuscript, and made critical revisions to the manuscript, as well as directing the animal and cell experiments. LW, PD and JC conceptualized the study, contributed to the formal analysis, the visualization of the study, and made critical revisions to the manuscript. JL and JF conceived and designed the experiments, analyzed the data and wrote the manuscript. All authors reviewed the manuscript. All the authors confirm the authenticity of all the raw data. All the authors have carefully reviewed the manuscript, and have read and approved the final manuscript.

Ethics approval and consent to participate

The present study was approved by the Ethics Committee of the Shanghai Outdo Biotech Co., Ltd, and was conducted in accordance with the ethical standards set out in the Declaration of Helsinki. All patients or their next of kin provided their informed consent prior to the study. The animals were housed under specific pathogen-free conditions at Zunyi Medical University. All animal experiments were performed according to the Guidelines for the Care and Use of Laboratory Animals (Ministry of Health, China, 1998). The experimental procedures were approved in accordance with the ethical guidelines of the Zunyi Medical University Laboratory Animal Care and Use Committee (permit no. 2018016).

Patient consent for publication

Not applicable.

Competing interests

The authors declare that they have no competing interests.

References

1. Morgan E, Arnold M, Gini A, Lorenzoni V, Cabasag CJ, Laversanne M, Vignat J, Ferlay J, Murphy N and Bray F: Global burden of colorectal cancer in 2020 and 2040: Incidence and mortality estimates from GLOBOCAN. Gut 72: 338-344, 2023.
2. Sung H, Ferlay J, Siegel RL, Laversanne M, Soerjomataram I, Jemal A and Bray F: Global Cancer Statistics 2020: GLOBOCAN Estimates of incidence and mortality worldwide for 36 cancers in 185 countries. CA Cancer J Clin 71: 209-249, 2021.
3. Krul MF, Elferink MAG, Kok NFM, Dekker E, Lansdorp-Vogelaar I, Meijer GA, Nagtegaal ID, Breekveldt ECH, Ruers TJM, van Leerdam ME and Kuhlmann KFD: Initial impact of national CRC screening on incidence and advanced colorectal cancer. Clin Gastroenterol Hepatol 21: 797-807, 2023.
4. Wele P, Wu X and Shi H: Sex-dependent differences in colorectal cancer: With a focus on obesity. Cells 11: 3688, 2022.
5. Barkley D, Moncada R, Pour M, Liberman DA, Dryg I, Werba G, Wang W, Baron M, Rao A, Xia B, *et al*: Cancer cell states recur across tumor types and form specific interactions with the tumor microenvironment. Nat Genet 54: 1192-1201, 2022.
6. Elhanani O, Ben-Uri R and Keren L: Spatial profiling technologies illuminate the tumor microenvironment. Cancer Cell 41: 404-420, 2023.

7. Luo H, Xia X, Huang LB, An H, Cao M, Kim GD, Chen HN, Zhang WH, Shu Y, Kong X, *et al*: Pan-cancer single-cell analysis reveals the heterogeneity and plasticity of cancer-associated fibroblasts in the tumor microenvironment. Nat Commun 13: 6619, 2022.
8. Xu W, Wu Y, Liu W, Anwaier A, Tian X, Su J, Huang H, Wei G, Qu Y, Zhang H and Ye D: Tumor-associated macrophage-derived chemokine CCL5 facilitates the progression and immunosuppressive tumor microenvironment of clear cell renal cell carcinoma. Int J Biol Sci 18: 4884-4900, 2022.
9. Chen D, Zhang X, Li Z and Zhu B: Metabolic regulatory crosstalk between tumor microenvironment and tumor-associated macrophages. Theranostics 11: 1016-1030, 2021.
10. Christofides A, Strauss L, Yeo A, Cao C, Charest A and Boussiotis VA: The complex role of tumor-infiltrating macrophages. Nat Immunol 23: 1148-1156, 2022.
11. Mantovani A, Allavena P, Marchesi F and Garlanda C: Macrophages as tools and targets in cancer therapy. Nat Rev Drug Discov 21: 799-820, 2022.
12. Pan Y, Yu Y, Wang X and Zhang T: Tumor-associated macrophages in tumor immunity. Front Immunol 11: 583084, 2020.
13. Cassetta L and Pollard JW: A timeline of tumour-associated macrophage biology. Nat Rev Cancer 23: 238-257, 2023.
14. Boutilier AJ and Elsawa SF: Macrophage polarization states in the tumor microenvironment. Int J Mol Sci 22: 6995, 2021.
15. Wang H, Yung MMH, Ngan HYS, Chan KKL and Chan DW: The impact of the tumor microenvironment on macrophage polarization in cancer metastatic progression. Int J Mol Sci 22: 6560, 2021.
16. Hwang I, Kim JW, Ylaya K, Chung EJ, Kitano H, Perry C, Hanaoka J, Fukuoka J, Chung JY and Hewitt SM: Tumor-associated macrophage, angiogenesis and lymphangiogenesis markers predict prognosis of non-small cell lung cancer patients. J Transl Med 18: 443, 2020.
17. Li H, Luo F, Jiang X, Zhang W, Xiang T, Pan Q, Cai L, Zhao J, Weng D, Li Y, *et al*: CircITGB6 promotes ovarian cancer cisplatin resistance by resetting tumor-associated macrophage polarization toward the M2 phenotype. J Immunother Cancer 10: e004029, 2022.
18. Ding CB, Yu WN, Feng JH and Luo JM: Structure and function of Gab2 and its role in cancer (Review). Mol Med Rep 12: 4007-4014, 2015.
19. Gong R, Li H, Liu Y, Wang Y, Ge L, Shi L, Wu G, Lyu J, Gu H and He L: Gab2 promotes acute myeloid leukemia growth and migration through the SHP2-Erk-CREB signaling pathway. J Leukoc Biol 112: 669-677, 2022.
20. Spohr C, Poggio T, Andrieux G, Schönberger K, Cabezas-Wallscheid N, Boerries M, Halbach S, Illert AL and Brummer T: Gab2 deficiency prevents Flt3-ITD driven acute myeloid leukemia in vivo. Leukemia 36: 970-982, 2022.
21. Zhang P, Chen Y, Gong M, Zhuang Z, Wang Y, Mu L, Wang T, Pan J, Liu Y, Xu J, *et al*: Gab2 ablation reverses the stemness of HER2-overexpressing breast cancer cells. Cell Physiol Biochem 50: 52-65, 2018.
22. Davis SJ, Sheppard KE, Anglesio MS, George J, Traficante N, Fereday S, Intermaggio MP, Menon U, Gentry-Maharaj A, Lubinski J, *et al*: Enhanced GAB2 expression is associated with improved survival in high-grade serous ovarian cancer and sensitivity to PI3K inhibition. Mol Cancer Ther 14: 1495-1503, 2015.
23. Duckworth C, Zhang L, Carroll SL, Ethier SP and Cheung HW: Overexpression of GAB2 in ovarian cancer cells promotes tumor growth and angiogenesis by upregulating chemokine expression. Oncogene 35: 4036-4047, 2016.
24. Hu X, He B, Zhou L, Xie H and Zheng S: Expression pattern and clinical significance of Gab2 protein in hepatocellular carcinoma. Clin Lab 62: 1087-1092, 2016.
25. Liu R, Sun Y, Chen S, Hong Y and Lu Z: FOXD3 and GAB2 as a pair of rivals antagonistically control hepatocellular carcinogenesis. FEBS J 289: 4536-4548, 2022.
26. Ding C, Luo J, Yu W, Gao S, Yang L, Chen C and Feng J: Gab2 is a novel prognostic factor for colorectal cancer patients. Int J Clin Exp Pathol 8: 2779-2786, 2015.
27. Horst B, Gruvberger-Saal SK, Hopkins BD, Bordone L, Yang Y, Chernoff KA, Uzoma I, Schwipper V, Liebau J, Nowak NJ, *et al*: Gab2-mediated signaling promotes melanoma metastasis. Am J Pathol 174: 1524-1533, 2009.
28. Livak KJ and Schmittgen TD: Analysis of relative gene expression data using real-time quantitative PCR and the 2(-Delta Delta C(T)) method. Methods 25: 402-408, 2001.
29. Adams SJ, Aydin IT and Celebi JT: GAB2-a scaffolding protein in cancer. Mol Cancer Res 10: 1265-1270, 2012.
30. Ding C, Luo J, Li L, Li S, Yang L, Pan H, Liu Q, Qin H, Chen C and Feng J: Gab2 facilitates epithelial-to-mesenchymal transition via the MEK/ERK/MMP signaling in colorectal cancer. J Exp Clin Cancer Res 35: 5, 2016.
31. Ding C, Luo J, Fan X, Li L, Li S, Wen K, Feng J and Wu G: Elevated Gab2 induces tumor growth and angiogenesis in colorectal cancer through upregulating VEGF levels. J Exp Clin Cancer Res 36: 56, 2017.
32. Wu K, Lin K, Li X, Yuan X, Xu P, Ni P and Xu D: Redefining tumor-associated macrophage subpopulations and functions in the tumor microenvironment. Front Immunol 11: 1731, 2020.
33. Guo X, Li T, Xu Y, Xu X, Zhu Z, Zhang Y, Xu J, Xu K, Cheng H, Zhang X and Ke Y: Increased levels of Gab1 and Gab2 adaptor proteins skew interleukin-4 (IL-4) signaling toward M2 macrophage-driven pulmonary fibrosis in mice. J Biol Chem 292: 14003-14015, 2017.
34. Cheng Y, Zhu Y, Xu J, Yang M, Chen P, Xu W, Zhao J, Geng L and Gong S: PKN2 in colon cancer cells inhibits M2 phenotype polarization of tumor-associated macrophages via regulating DUSP6-Erk1/2 pathway. Mol Cancer 17: 13, 2018.
35. Gao J, Liang Y and Wang L: Shaping polarization of tumor-associated macrophages in cancer immunotherapy. Front Immunol 13: 888713, 2022.
36. Kashfi K, Kannikal J and Nath N: Macrophage reprogramming and cancer therapeutics: Role of iNOS-derived NO. Cells 10: 3194, 2021.
37. Zhang Q and Sioud M: Tumor-associated macrophage subsets: Shaping polarization and targeting. Int J Mol Sci 24: 7493, 2023.
38. Bingle L, Brown NJ and Lewis CE: The role of tumour-associated macrophages in tumour progression: Implications for new anticancer therapies. J Pathol 196: 254-265, 2002.
39. Wang X, Yuwen TJ, Zhong Y, Li ZG and Wang XY: A new method for predicting the prognosis of colorectal cancer patients through a combination of multiple tumor-associated macrophage markers at the invasive front. Heliyon 9: e13211, 2023.
40. Shen T, Liu JL, Wang CY, Rixiati Y, Li S, Cai LD, Zhao YY and Li JM: Targeting erbin in B cells for therapy of lung metastasis of colorectal cancer. Signal Transduct Target Ther 6: 115, 2021.
41. Hou J, Zhang Y and Zhu Z: Gene heterogeneity in metastasis of colorectal cancer to the lung. Semin Cell Dev Biol 64: 58-64, 2017.
42. Malki A, ElRuz RA, Gupta I, Allouch A, Vranic S and Al Moustafa AE: Molecular mechanisms of colon cancer progression and metastasis: Recent insights and advancements. Int J Mol Sci 22: 130, 2020.
43. Ye Q, Cai W, Zheng Y, Evers BM and She QB: ERK and AKT signaling cooperate to translationally regulate survivin expression for metastatic progression of colorectal cancer. Oncogene 33: 1828-1839, 2014.
44. Hijazi M, Casado P, Akhtar N, Alvarez-Teijeiro S, Rajeeve V and Cutillas PR: eEF2K activity determines synergy to cotreatment of cancer cells with PI3K and MEK inhibitors. Mol Cell Proteomics 21: 100240, 2022.
45. Cheng J, Zhong Y, Chen S, Sun Y, Huang L, Kang Y, Chen B, Chen G, Wang F, Tian Y, *et al*: Gab2 mediates hepatocellular carcinogenesis by integrating multiple signaling pathways. FASEB J 31: 5530-5542, 2017.
46. Wang Y, Sheng Q, Spillman MA, Behbakht K and Gu H: Gab2 regulates the migratory behaviors and E-cadherin expression via activation of the PI3K pathway in ovarian cancer cells. Oncogene 31: 2512-2520, 2012.